Cerebral Cortex October 2015;25:3699–3712
doi:10.1093/cercor/bhu231
Advance Access publication September 26, 2014

# Endocannabinoids Induce Lateral Long-Term Potentiation of Transmitter Release by Stimulation of Gliotransmission

Marta Gómez-Gonzalo[1], Marta Navarrete[1,5], Gertrudis Perea[1], Ana Covelo[2], Mario Martín-Fernández[2], Ryuichi Shigemoto[3], Rafael Luján[4] and Alfonso Araque[1,2]

[1]Instituto Cajal, CSIC, Madrid 28002, Spain, [2]Department of Neuroscience, University of Minnesota, Minneapolis, MN 55455, USA, [3]Division of Cerebral Structure, National Institute for Physiological Sciences, Okazaki 444-8787, Japan, [4]Instituto de Investigación en Discapacidades Neurológicas (IDINE), Departamento de Ciencias Médicas, Facultad de Medicina, Universidad Castilla-La Mancha, Albacete 02006, Spain and [5]Current address: Department of Neurobiology, Centro de Biología Molecular "Severo Ochoa," (CSIC/UAM), Madrid, Spain

Address correspondence to Prof. Alfonso Araque, Department of Neuroscience, University of Minnesota, 4-110 Wallin Medical Biosciences Building, 2101 6th Street SE, Minneapolis, MN 55455, USA. Email: araque@umn.edu

Marta Gómez-Gonzalo, Marta Navarrete, Gertrudis Perea, and Ana Covelo contributed equally to this work.

**Endocannabinoids (eCBs) play key roles in brain function, acting as modulatory signals in synaptic transmission and plasticity. They are recognized as retrograde messengers that mediate long-term synaptic depression (LTD), but their ability to induce long-term potentiation (LTP) is poorly known. We show that eCBs induce the long-term enhancement of transmitter release at single hippocampal synapses through stimulation of astrocytes when coincident with postsynaptic activity. This LTP requires the coordinated activity of the 3 elements of the tripartite synapse: 1) eCB-evoked astrocyte calcium signal that stimulates glutamate release; 2) postsynaptic nitric oxide production; and 3) activation of protein kinase C and presynaptic group I metabotropic glutamate receptors, whose location at presynaptic sites was confirmed by immunoelectron microscopy. Hence, while eCBs act as retrograde signals to depress homoneuronal synapses, they serve as lateral messengers to induce LTP in distant heteroneuronal synapses through stimulation of astrocytes. Therefore, eCBs can trigger LTP through stimulation of astrocyte–neuron signaling, revealing novel cellular mechanisms of eCB effects on synaptic plasticity.**

**Keywords:** astrocytes, endocannabinoid signaling, LTP, mGluRs, nitric oxide

## Introduction

The endocannabinoid (eCB) system comprises 2 cannabinoid receptors, type 1 (CB1) and type 2 (CB2), and the endogenous ligands, eCB. eCBs retrogradely modulate synaptic transmission widely throughout the central nervous system playing relevant neuromodulatory roles in multiple physiological processes (Freund et al. 2003; Chevaleyre et al. 2006). They are released from postsynaptic neurons, activate presynaptic $CB_1$ cannabinoid receptors, and reduce transmitter release either transiently (endocannabinoid-mediated short-term depression; eCB-STD) or persistently (endocannabinoid-mediated long-term depression; eCB-LTD) (Kreitzer and Regehr 2001a; Alger 2002; Wilson and Nicoll 2002; Freund et al. 2003; Chevaleyre et al. 2006; Heifets and Castillo 2009), and are responsible for most of the behavioral effects of cannabinoids (Maldonado et al. 2006). Recent studies in goldfish (Cachope et al. 2007), lampreys spinal cord (Song et al. 2012), and rodent hippocampal slices (Navarrete and Araque 2010) have reported that CB1R activation can transiently enhance neurotransmission. Although the role of eCB signaling in synaptic plasticity is thought to exclusively induce long-term synaptic depression (LTD), its involvement in the long-term potentiation (LTP) of synaptic transmission is still poorly known (Xu et al. 2012).

Astrocytes have emerged as active elements directly involved in synaptic physiology. They respond with $Ca^{2+}$ elevations to neurotransmitters released by neurons and modulate neuronal excitability and synaptic transmission by releasing gliotransmitters (Araque et al. 2001; Nedergaard et al. 2003; Volterra and Meldolesi 2005; Haydon and Carmignoto 2006; Perea et al. 2009; Parpura and Zorec 2010; Singh et al. 2014), hence being active elements of synaptic function at tripartite synapses (Araque et al. 1999; Perea et al. 2009). While eCBs released by neurons exert their effects at short distances [<20 µm (Wilson and Nicoll 2001; Piomelli 2003; Chevaleyre and Castillo 2004; Chevaleyre et al. 2006; Navarrete and Araque 2010)], the possible long-range effects of eCBs signaling on synaptic plasticity through astrocyte network stimulation remain largely unknown. The demonstration that hippocampal astrocytes express functional CB1Rs, which increase astrocyte $Ca^{2+}$ levels and stimulate glutamate release (Navarrete and Araque 2008), suggests that astrocytes are directly involved in the eCB intercellular signaling as well as in its functional consequences on synaptic transmission. Indeed, a more recent study has shown that eCB-mediated neuron-to-astrocyte signaling lead to the short-term potentiation of synaptic transmission in hippocampal synapses (Navarrete and Araque 2010). Furthermore, the eCB-astrocyte signaling has been related with cortical LTD (Min and Nevian 2012) and the impairment of spatial working memory and hippocampal LTD induced by exogenous cannabinoids (Han et al. 2012). However, despite these studies revealing the role of eCB-astrocyte signaling on synaptic depression processes, the consequences and underlying molecular mechanisms of eCB-astrocyte signaling on long-lasting enhancement of synaptic activity remain largely unknown.

Our previous studies have demonstrated that calcium elevations in astrocytes elicited by $Ca^{2+}$ uncaging or eCBs released from neurons induce a transient synaptic potentiation of hippocampal synaptic transmission (Perea and Araque 2007; Navarrete and Araque 2010), and that pairing astrocyte $Ca^{2+}$ uncaging and mild postsynaptic depolarization can induce long-term changes in synaptic efficacy. Using electrophysiological and $Ca^{2+}$ imaging techniques in mouse brain slices, we have investigated whether eCBs released from neurons, acting as endogenous signals that activate astrocytes (Navarrete and Araque 2008), could induce the LTP of synaptic transmission.

We have also investigated the underlying signaling pathways and molecular mechanisms responsible for the LTP mediated by the coincidence of astrocytic and postsynaptic activities. Here, we show that the coincidence of eCB signaling and postsynaptic activity leads to the eCB-induced long-term potentiation (eLTP) at single synapses in neurons relatively distant from the eCBs source. This form of LTP results from the coincidence of signaling events through the concerted activity of the tripartite synapse: 1) eCB-evoked astrocyte $Ca^{2+}$ signal that stimulates glutamate release; 2) postsynaptic nitric oxide (NO) production; and 3) activation of presynaptic metabotropic glutamate receptors (group I mGluRs) and protein kinase C (PKC). Therefore, eCBs induce lateral LTP of synaptic transmission in relatively distant synapses through stimulation of CB1Rs in astrocytes. These results contribute to the growing body of evidence highlighting the role of astrocytes in long-term synaptic modulation.

## Materials and Methods

### *Ethics Statement*

All the procedures for handling and sacrificing animals followed the European Commission guidelines (2010/63/EU).

### *Hippocampal Slice Preparation*

Hippocampal slices were obtained from C57BL/6 mice (13–18 days old). In some cases, slices from CB1 receptor knockout mice and $IP_3R2$ knockout mice, generously donated by Dr A. Zimmer and Dr J. Chen, respectively, were used (Zimmer et al. 1999; Li et al. 2005). Animals were anesthetized and decapitated. The brain was rapidly removed and placed in ice-cold artificial cerebrospinal fluid (ACSF). Slices (350–400 μm thick) were incubated (>30 min) at room temperature (21–24 °C) in ACSF containing (in mM): NaCl 124, KCl 2.69, $KH_2PO_4$ 1.25, $MgSO_4$ 2, $NaHCO_3$ 26, $CaCl_2$ 2, and glucose 10, and was gassed with 95% $O_2$/5% $CO_2$ (pH = 7.3). Slices were transferred to an immersion recording chamber and superfused at 2 mL/min with gassed ACSF including 0.05 mM Picrotoxin and 5 μM (2*S*)-3-[[(1*S*)-1-(3,4-dichlorophenyl)ethyl]amino-2-hydroxypropyl](phenylmethyl)phosphonic acid hydrochloride (CGP 55845) to block $GABA_A$ and $GABA_B$ receptors, respectively. Cells were visualized under an Olympus BX50WI microscope (Olympus Optical, Tokyo, Japan).

### *Electrophysiology*

Simultaneous electrophysiological whole-cell patch-clamp recordings from 2 CA1 pyramidal neurons (distance of the somas: 60–150 μm) were made. Patch electrodes had resistances of 3–10 MΩ when filled with the internal solution containing (in mM): K-gluconate 135, KCl 10, HEPES 10, $MgCl_2$ 1, ATP-$Na_2$ 2 (pH 7.3 adjusted with KOH; osmolality 280–290 mOsm/L). Recordings were obtained with PC-ONE amplifiers (Dagan Instruments, Minneapolis, MN, USA). Membrane potential was held at −70 mV. Series and input resistances were monitored throughout the experiment using a −5-mV pulse. Recordings were considered stable when the series and input resistances, resting membrane potential, and stimulus artifact duration did not change >20%. Cells that did not meet these criteria were discarded. Signals were fed to a Pentium-based PC through a DigiData 1440A interface board. Signals were filtered at 1 kHz and acquired at 10-kHz sampling rate. The pCLAMP 10.2 (Axon instruments) software was used for stimulus generation, data display, acquisition, and storage. In some experiments, astrocytes were patched with 4–9 MΩ electrodes filled with an intracellular solution containing (in mM): $KMeSO_4$ 100, KCl 50, HEPES 10, ATP-$Na_2$ 2 (pH 7.3 adjusted with KOH; osmolality 280–290 mOsm/L). Since the synaptic potentiation induced in experiments performed at room temperature (21–24 °C) and at 30–32 °C was not significantly different (see Fig. 1*E*), experiments were performed at room temperature, unless stated otherwise.

### *Synaptic Stimulation*

Theta capillaries filled with ACSF were used for bipolar minimal stimulation. Electrodes were connected to a stimulator S-910 through an isolation unit and placed in the "stratum radiatum" to stimulate Schaffer collaterals (SCs). Single pulses (250-μs duration) or paired pulses (50-ms interval) were continuously delivered at 0.33 Hz. Excitatory postsynaptic currents (EPSCs) were simultaneously recorded from the eCB-releasing neuron (homoneuronal synapses) and from the postsynaptic neuron (heteroneuronal synapses). Stimulus intensity (0.1–10 mA) was adjusted to meet the conditions that putatively stimulate single or very few presynaptic fibers [cf. (Raastad 1995; Isaac et al. 1996; Perea and Araque 2007; Navarrete and Araque 2010)]. Recordings that did not meet these criteria and did not show amplitude stability of basal EPSCs were rejected. The synaptic parameters analyzed were: synaptic efficacy (mean peak amplitude of all responses including failures); synaptic potency (mean peak amplitude of the successes); probability of release (Pr, ratio between number of successes vs. total number of stimuli); and paired-pulse facilitation ratio (PPF = 2nd EPSC/1st EPSC). Synaptic plasticity changes were determined from 180 stimuli before (basal) and 60 min after stimulus (i.e., depolarization of the eCB-releasing neuron or astrocyte $Ca^{2+}$ uncaging). To illustrate the time course, synaptic parameters were grouped in 3-min bins. EPSC amplitude was determined as the peak current amplitude (2–9 ms after stimulus) minus the mean baseline current (20–30 ms before stimulus). A response was considered a failure if the amplitude of the current was <3 times the standard deviation of the baseline current, and was verified by visual inspection.

All the experiments were performed in an unbiased form and a blind design whenever possible. The experimental paradigm used was based on single-cell stimulation and single-synapse recording, which presents the limitation that some specific recorded synapses may not be under the direct influence of the stimulated cell (pyramidal neuron or astrocyte; cf. Perea and Araque 2007; Navarrete and Araque 2010). Consistent with this idea, although a subset of the recorded single synapses (8 of 12; i.e., around 66.6%) showed eLTP, in the present study synapses were not selected according to their susceptibility to modulation, and data correspond to average values of all the recorded synapses in each condition. Consequently, while the average values underestimate the actual magnitude of the modulatory phenomena at a single synapse, they validate the relevance of the phenomenon on the overall synaptic activity.

The following "paired depolarizing protocol" was used: The termed postsynaptic neuron was depolarized to −30 mV for 3 min to mimic postsynaptic activity. After the first minute, the termed eCB-releasing neuron was depolarized to 0 mV for 5 s to stimulate eCB release. SC stimulation was interrupted during the paired depolarizing protocol, and resumed afterward. When indicated, theta burst stimulation (TBS) stimulation [4 trains at 5 Hz of 4 stimuli (at 40 Hz) delivered 10 times at 0.1 Hz] applied by an independent glass pipette to independent SC pathways was used to synaptically induce postsynaptic depolarization recorded in current-clamp mode, and 50 s after initiating the TBS paradigm the eCB-releasing neuron was depolarized to 0 mV for 5 s. The independence of the SC pathways stimulated by single synapse and conventional TBS stimuli was confirmed by stimulating both pathways simultaneously with time intervals of 50 ms and observing no cross-facilitation of the corresponding EPSCs.

The slow $Ca^{2+}$-activated $K^+$ current ($sI_{AHP}$) was evoked by 200-ms depolarizing pulses (from −60 to 20 mV). The $sI_{AHP}$ magnitude was quantified from the area under the current trace, measured 60–100 ms after the end of the pulse (Martin et al. 2001).

### *$Ca^{2+}$ Imaging*

$Ca^{2+}$ levels in astrocytes located in the stratum radiatum of the CA1 region of the hippocampus were monitored by fluorescence microscopy using the $Ca^{2+}$ indicator fluo-4 (Molecular Probes, Eugene, OR, USA). $Ca^{2+}$ signal was monitored from cells located within a 150-μm wide region around the stimulated neuron and perpendicular to the "stratum pyramidale." Slices were incubated with fluo-4 AM (2–5 μL of 2 mM dye were dropped over the hippocampus, attaining a final concentration of 2–10 μM and 0.01% of pluronic) for 20–30 min at room

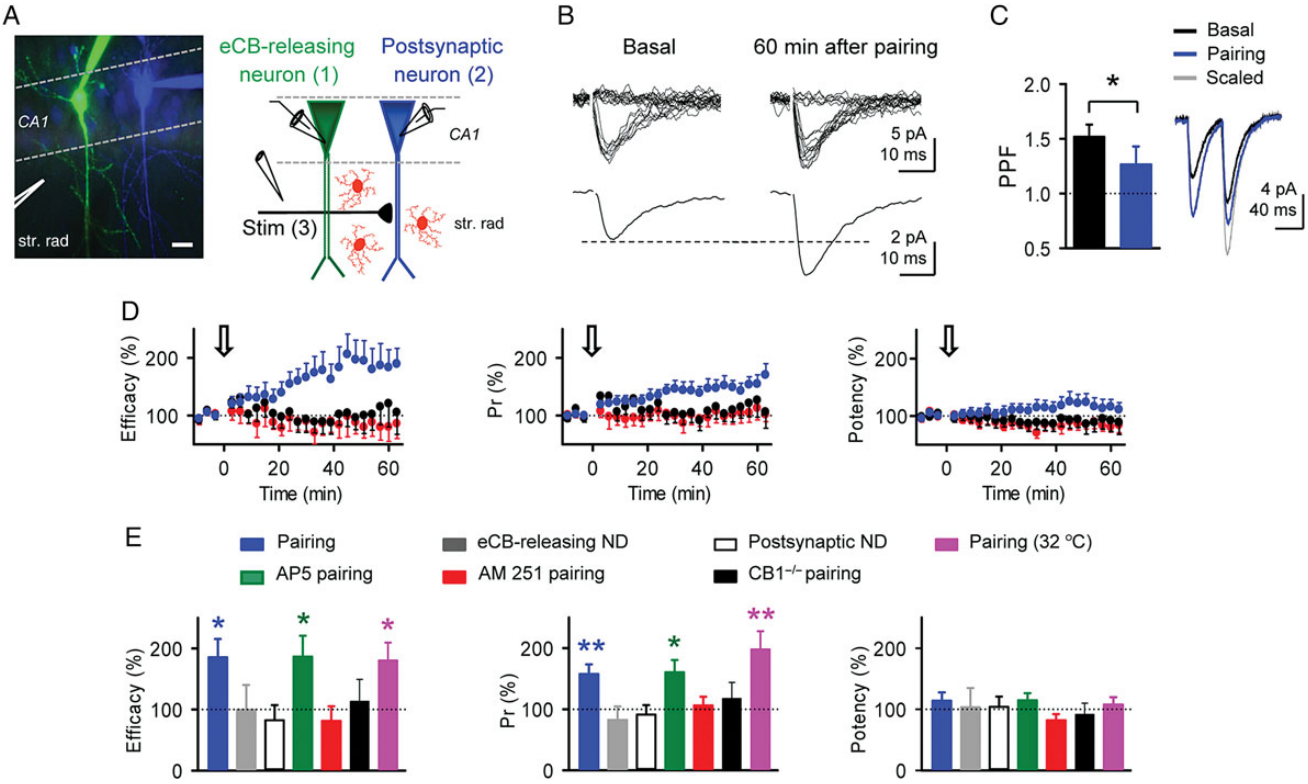


**Figure 1.** Endocannabinoid signaling induces LTP of transmitter release at single hippocampal synapses. (*A*) Left, false-color image of 2 CA1 pyramidal neurons filled with AlexaFluor 488 (1, green) and sulforhodamine B (2, blue) through the recording pipettes, and stimulus pipette (3). Scale bar, 10 μm. Right, schematic drawing of the experimental approach depicting paired recordings and the minimal stimulating electrode. (*B*) Representative synaptic responses evoked by minimal stimulation showing regular EPSC amplitudes and failures of synaptic transmission (20 stimuli; top traces) and averaged EPSCs ($n = 60$ stimuli, including successes and failures; bottom traces) before (basal) and 60 min after pairing protocol. (*C*) Averaged EPSCs evoked by paired-pulse stimulation and PPF ratio before (black) and 60 min after pairing protocol (blue). Gray trace is the scaled trace of the basal EPSC. (*D*) Synaptic efficacy, probability of neurotransmitter release (Pr) and synaptic potency versus time after the pairing protocol in control (blue circles; $n = 12$), in the presence of the CB1R antagonist AM251 (2 μM; red circles; $n = 5$), and in slices from CB1R$^{-/-}$ mice (black circles; $n = 6$). Zero time corresponds to the beginning of neuronal depolarizations (arrow) (as in all other figures). (*E*) Relative changes of synaptic parameters 60 min after pairing protocol in control ($n = 12$), unpaired depolarization of eCB-releasing neuron ($n = 8$) or postsynaptic neuron ($n = 6$), after pairing protocol in AP5 ($n = 10$), after pairing protocol in AM251 ($n = 5$), in CB1R $^{-/-}$ mice ($n = 6$), and after pairing at 32 °C ($n = 10$). ND, neuronal depolarization. *$P < 0.05$, **$P < 0.01$. Data are represented as mean ± SEM (as in all other figures).

temperature. In these conditions, most of the cells loaded were astrocytes (Kang et al. 1998; Parri et al. 2001; Araque et al. 2002; Nett et al. 2002; Perea and Araque 2005) as confirmed in some cases by their electrophysiological properties. Astrocytes were imaged using a CCD camera (Retiga EX; Qimaging, Canada). Cells were illuminated during 200–500 ms with a xenon lamp at 490 nm using a monochromator Polychrome V (T.I.L.L. Photonics, Planegg, Germany), and images were acquired every 1 s. The monochromator Polychrome V and the CCD camera were controlled and synchronized by the IP Lab software (BD Biosciences, MD, USA) that was also used for quantitative epifluorescence measurements. $Ca^{2+}$ variations, termed $Ca^{2+}$ spikes, were recorded at the soma of the cells and estimated as changes of the fluorescence signal over baseline ($\Delta F/F_0$), and cells were considered to respond to the stimulation when $\Delta F/F_0$ increased 3 times the standard deviation of the baseline for at least 2 consecutive images and with a delay ≤15 s after the stimulation. Neuronal $Ca^{2+}$ variations were recorded with patch pipettes filled with the internal solution containing 50 μM fluo-4 to monitor $Ca^{2+}$ levels, and estimated by same criteria as for astrocyte $Ca^{2+}$ signals.

Astrocyte $Ca^{2+}$ responses were quantified analyzing the probability of occurrence of $Ca^{2+}$ spikes; this is, detecting the onset of $Ca^{2+}$ elevations ($Ca^{2+}$ spikes) during the recording period and grouped in 5-s bins from 6 to 18 astrocytes in the field of view. Values of 0 and 1 were assigned for bins showing no response and $Ca^{2+}$ spike, respectively, to obtain the $Ca^{2+}$ spike probability index. To test the effects on $Ca^{2+}$ spike probability (Pr) under different conditions, the respective mean basal (15 s before the paired depolarizing protocol) and maximum $Ca^{2+}$ spike probability (15 s after the paired depolarizing protocol) from different slices were averaged and compared. Slices from at least 4 independent animals per condition were used.

### *$Ca^{2+}$ Uncaging by UV-flash Photolysis*

In photostimulation experiments, single astrocytes were recorded with patch pipettes filled with the internal solution containing 5 mM NP-EGTA (and 50 μM fluo-4 to monitor $Ca^{2+}$ levels). $Ca^{2+}$ uncaging was achieved by delivering train pulses (1-ms duration, 6–15 mW) of UV light (340–380 nm) at 2 Hz during 10 s to the soma and processes of the recorded astrocyte (optical window of 15–25 μm diameter), inducing reliable $Ca^{2+}$ elevations, using a flash photolysis system (Rapp OptoElectronic, Hamburg, Germany). Control experiments were performed by delivering UV photostimulating astrocytes not loaded with NP-EGTA. No astrocyte $Ca^{2+}$ signal or synaptic transmission parameter changes were observed (cf. Perea and Araque 2007; Navarrete et al. 2012).

### *Electron Microscopy*

Immunohistochemical reactions for electron microscopy were performed using the pre-embedding immunogold method (Lujan et al. 1996). C57BL/6 mice (18 days old) were anesthetized and transcardially perfused with ice-cold fixative containing 4% paraformaldehyde, 0.05% glutaraldehyde, and 15% (v/v) saturated picric acid made up in 0.1 M phosphate buffer (PB, pH 7.4). After perfusion, brains were removed, washed thoroughly in 0.1 M PB, and cut on a Vibratome (Leica V1000) obtaining coronal 60-μm-thick sections. Free-floating

sections were incubated in 10% (v/v) NGS diluted in Tris-buffered saline solution. Sections were then incubated with pan-mGluR1 antibodies at a final protein concentration of 3–5 μg/mL diluted in Tris-buffered saline solution containing 1% (v/v) NGS. After several washes in Tris-buffered saline solution, sections were incubated with goat anti-mouse IgG coupled to 1.4-nm gold (Nanoprobes, Inc., Stony Brook, NY, USA). Sections were postfixed in 1% (v/v) glutaraldehyde and washed in double distilled water, followed by silver enhancement of the gold particles with a HQ Silver kit (Nanoprobes, Inc.). Sections were then treated with osmium tetraoxide (1% in 0.1 M PB), block-stained with uranyl acetate, dehydrated in graded series of ethanol, and flat-embedded on glass slides in Durcupan (Fluka) resin. Regions of interest were cut at 70–90 nm on an ultramicrotome (Reichert Ultracut E, Leica, Austria) and collected single slot pioloform-coated copper grids. Ultrastructural analyses were performed in a Jeol-1010 electron microscope (Jeol, Tokio, Japan). The rabbit polyclonal antibody $mGlu_1$ recognize an extracellular epitope that is present in all isoforms of mGluR1. The specificity of this antibody has been described previously (Lujan et al. 1996), and further characterization on the presynaptic labeling is presented here (Fig. 6*G*) using mGluR1b rescue mice (generously donated by Dr Atsu Aiba), in which the mGluR1b isoform is rescue in Purkinje cells, but is basically an mGluR1 KO mice in the rest of the brain (Kishimoto et al. 2002).

To establish the relative frequency of mGluR1 immunoreactivity in the stratum radiatum of the CA1 region, we used 60-μm coronal slices processed for pre-embedding immunogold immunohistochemistry. The procedures were similar to those used previously (Lujan et al. 1996). Briefly, for each of 3 young adult animals, 3 samples of tissue were obtained for preparation of embedding blocks, totaling $n = 9$ blocks. To minimize false negatives, electron microscopic serial ultrathin sections were cut close to the surface of each block, as immunoreactivity decreased with depth. We estimated the quality of immunolabeling by always selecting areas with optimal gold labeling at approximately the same distance from the cutting surface, which was defined within 5–10 μm from the surface. Randomly selected areas were then photographed from the selected ultrathin sections and printed with a final magnification of ×50 000. Quantification of immunogold labeling was carried out in reference areas totaling ~1000 $\mu m^2$. Immunoparticles identified in each reference area and present in different subcellular compartments (dendritic spines, dendritic shafts, and axon terminals) were counted. Data were expressed as percentage of immunoparticles in each subcellular compartment. We also counted the number of excitatory synapses labeled and unlabeled for mGluR1, both at postsynaptic and presynaptic sites.

### *Drugs and Chemicals*

*N*-(Piperidin-1-yl)-5-(4-iodophenyl)-1-(2,4-dichlorophenyl)-4-methyl-1H-pyrazole-3-carboxamide (AM-251); 2-methyl-6-(phenylethynyl) pyridine hydrochloride (MPEP), (*S*)-(+)-α-amino-4-carboxy-2-methyl benzeneacetic acid (LY367385), CGP 55845, and bisindolylmaleimide 1 (BIS I) were purchased from Tocris Cookson (Bristol, UK); fluo-4 AM and *o*-nitrophenyl EGTA, tetrapotassium salt (NP-EGTA) from Molecular Probes; and (S)-3,5-Dihydroxyphenylglycine (DHPG) from Ascent Scientific (Bristol, UK). All other drugs were from Sigma.

### *Statistical Analysis*

Data are expressed as mean ± standard error of the mean (SEM). Normality test (Shapiro–Wilk test) was applied to the data before running statistical tests. Based on that, data were analyzed using parametric (Student's *t*-test, $\alpha = 0.05$) and nonparametric tests (Wilcoxon signed-rank test) as appropriate. Statistical differences were established with $P < 0.05$ (*), $P < 0.01$ (**), and $P < 0.001$ (***).

## Results

### *Endocannabinoid Signaling Induces LTP of Transmitter Release in Heteroneuronal Synapses*

To investigate whether eCB signaling could induce LTP of synaptic plasticity through astrocyte network activation, we recorded pairs of hippocampal CA1 pyramidal neurons (>60 μm apart), recorded astrocyte $Ca^{2+}$ levels, and monitored SC-evoked synaptic transmission at single synapses (using the minimal stimulation technique that activates single or very few presynaptic fibers; see Materials and Methods; Fig. 1*A*,*B*). We used the following paired depolarizing protocol: We depolarized one neuron (termed eCB-releasing neuron, and whose synapses are called homoneuronal synapses) to 0 mV for 5 s to stimulate eCB release (Kreitzer and Regehr 2001a; Wilson and Nicoll 2001; Ohno-Shosaku et al. 2002; Chevaleyre and Castillo 2004; Navarrete and Araque 2008, 2010) and monitored synaptic activity in the other neuron (termed postsynaptic neuron, and whose synapses are called heteroneuronal synapses), which was mildly depolarized to −30 mV to mimic postsynaptic activity (cf. Perea and Araque 2007). We focused our study on heteroneuronal synapses, because homoneuronal synapses onto the eCB-releasing neuron are known to undergo CB1R-mediated synaptic depression (see Fig. 3*A*,*B*; cf. Kreitzer and Regehr 2001a; Ohno-Shosaku et al. 2001; Chevaleyre et al. 2006; Navarrete and Araque 2010). The paired depolarizing protocol induced a long-lasting enhancement of synaptic transmission in 8 of 12 heteroneuronal synapses. The synaptic efficacy increased from $-4.8 \pm 0.6$ to $-7.8 \pm 1.7$ pA ($n = 12$; $P = 0.016$) which resulted from the increase of the probability of release (Pr; from $0.50 \pm 0.05$ to $0.69 \pm 0.06$; $n = 12$; $P = 0.021$) without changes in the synaptic potency (from $-11.1 \pm 0.9$ to $-11.7 \pm 1.5$ pA; $n = 12$; $P = 0.719$) (Fig. 1*D*,*E*). These changes, which were similarly observed at room temperature and more physiological temperatures (30–32 °C), were associated with a decrease in the PPF (from $1.52 \pm 0.11$ to $1.27 \pm 0.16$; $n = 8$; $P = 0.015$; Fig. 1*C*), indicating a presynaptic mechanism of action, which is also consistent with changes in Pr but not in synaptic potency.

These long-term synaptic changes were absent when either the mild depolarization of the postsynaptic neuron or the depolarization of the eCB-releasing neuron were delivered alone ($n = 6$ and 8, respectively; Fig. 1*E*; cf. Perea and Araque 2007; Navarrete and Araque 2010) and they were not prevented in the presence of the NMDAR antagonist AP5 (50 μM) ($n = 10$; Fig. 1*E*), indicating that NMDARs were not involved in this form of LTP. They were also absent when the paired depolarizing protocol was applied in the presence of the CB1R antagonist AM251 (2 μM) or in transgenic mice lacking CB1Rs ($n = 5$ and 6, respectively) (Fig. 1*D*,*E*), indicating that these changes were mediated by the coincidence of eCBs and postsynaptic signaling. Taken together, these results indicate that eCBs released from the eCB-releasing neuron can trigger the long-term potentiation (eLTP) of transmitter release in heteroneuronal synapses of relatively distant neurons when it coincides with postsynaptic activity.

To test whether eLTP could be triggered by a more physiological stimulus, instead of artificially depolarizing the postsynaptic neuron to −30 mV, we stimulated independent SC pathways using a theta burst paradigm (4 trains at 5 Hz of 4 stimuli at 40 Hz were delivered 10 times at 0.1 Hz). TBS, delivered at intensities that depolarized the postsynaptic neuron below the action potential threshold, did not evoke synaptic potentiation per se, but it induced lateral eLTP when paired with the depolarization of the eCB-releasing neuron ($n = 6$; Fig. 2*B*–*D*). These results indicate that lateral eLTP can be evoked under more physiological conditions.

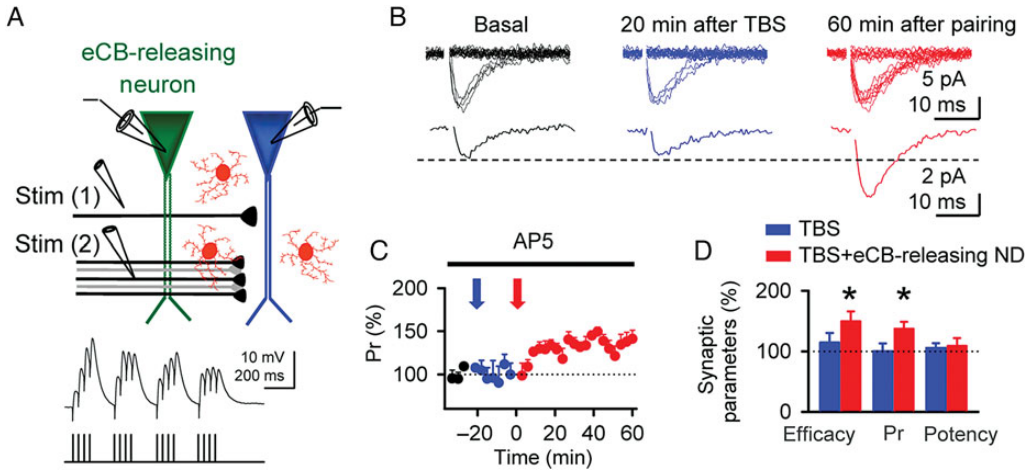


**Figure 2.** Pairing endocannabinoid signaling and synaptically induced postsynaptic depolarization induces LTP. (*A*) Schematic drawing of the experimental approach depicting paired recordings and the minimal (1) and TBS (2) stimulating electrodes. (*B*) Representative synaptic responses (20 stimuli; top traces) and averaged EPSCs (20 stimuli, including successes and failures; bottom traces) recorded from the postsynaptic neuron in basal conditions (black), 20 min after TBS alone (blue), and 60 min after pairing TBS with the depolarization of the eCB-releasing neuron (red). These experiments were performed in the presence of AP5 to prevent NMDARs-mediated plasticity evoked by TBS stimulation. (*C*) Relative changes of Pr in basal conditions (black circles), after TBS alone (blue), and after pairing TBS with the depolarization of the eCB-releasing neuron (red). Blue arrow indicates TBS alone and red arrow indicates pairing of TBS with the depolarization of the eCB-releasing neuron. Zero time corresponds to the beginning of the paired protocol. (*D*) Relative change of synaptic parameters 20 min after TBS protocol and 60 min after paired protocol ($n = 6$). *$P < 0.05$.

### *Astrocyte Signaling: eLTP Requires Astrocyte $Ca^{2+}$ Elevations*

Because eCBs can modulate neurotransmission through stimulation of CB1R-mediated astrocyte $Ca^{2+}$ elevations (Navarrete and Araque 2010; Min and Nevian 2012), we tested the involvement of the astrocyte $Ca^{2+}$ signal in the generation of eLTP. We used hippocampal slices from transgenic mice lacking the inositol-1,4,5-trisphosphate($IP_3$)-receptor type 2 ($IP_3R2^{-/-}$ mice) (Li et al. 2005), which is the primary functional $IP_3$ receptor expressed by astrocytes that mediates G protein-mediated intracellular $Ca^{2+}$ mobilization (Petravicz et al. 2008; Di Castro et al. 2011; Navarrete et al. 2012). First, we assessed whether the eCB release evoked by neuronal depolarization was affected in these mice by monitoring the depolarization-induced suppression of excitation (DSE) in homoneuronal synapses, a well-known phenomenon mediated by presynaptic CB1Rs (Kreitzer and Regehr 2001a; Ohno-Shosaku et al. 2002; Chevaleyre et al. 2006; Navarrete and Araque 2010). The amplitude of the DSE was not significantly different in wild-type and $IP_3R2^{-/-}$ mice ($n = 6$ and 6, respectively, Fig. 3*A*,*B*), indicating that the eCB release machinery and neuronal CB1R activation is preserved in these knockout animals. In contrast, while the neuronal depolarization elevated astrocyte $Ca^{2+}$ in slices from wild-type mice (47 of 74 astrocytes from 8 slices) (cf. Navarrete and Araque 2008, 2010), it failed to elevate astrocyte $Ca^{2+}$ in $IP_3R2^{-/-}$ mice (only 1 of 55 astrocytes from 8 slices displayed $Ca^{2+}$ elevations) (Fig. 3*C*–*E*). Accordingly, the eLTP observed in slices from wild-type mice was largely suppressed in $IP_3R2^{-/-}$ mice ($n = 8$; Fig. 3*F*–*H*). Therefore, these results indicate that eLTP requires astrocyte $Ca^{2+}$ elevations.

To further confirm the involvement of astrocyte $Ca^{2+}$ signal on eLTP, we stimulated astrocytes downstream the eCB signaling, by loading astrocytes with the $Ca^{2+}$ cage NP-EGTA (5 mM), which upon UV light stimulation reliably elevated astrocyte $Ca^{2+}$ in slices from both wild-type and $IP_3R2^{-/-}$ mice (Fig. 4*A*, *B*). Pairing the mild postsynaptic depolarization (to −30 mV) and the astrocyte $Ca^{2+}$ uncaging resulted in the LTP of transmitter release in slices from wild-type and $IP_3R2^{-/-}$ mice ($n = 6$ and 6, respectively, Fig. 4*C*,*D*; cf. Perea and Araque 2007). These results indicate that eCB effects can be mimicked by astrocyte $Ca^{2+}$ uncaging and that the signaling pathways downstream the astrocyte $Ca^{2+}$ signal involved in this form of LTP are unaffected in $IP_3R2^{-/-}$ mice. Therefore, when coincident with the postsynaptic activity, the astrocyte $Ca^{2+}$ signal is necessary to induce LTP.

### *Postsynaptic Signaling: eLTP Requires NO Production in the Postsynaptic Neuron*

Because eLTP is expressed presynaptically as an enhancement of transmitter release probability and requires the postsynaptic depolarization, we aimed to identify the retrograde signal that being released from the postsynaptic cell impact the presynaptic function. A likely candidate is NO because it is an intercellular messenger that may act retrogradely and is involved in synaptic plasticity (Schuman and Madison 1991, 1994; Hawkins et al. 1998). When slices were incubated with the NO scavenger PTIO (100 μM; Fig. 5*A*), the eCB-induced astrocyte $Ca^{2+}$ signal was unaffected ($n = 98$ astrocytes from $n = 7$ slices: Fig. 5*B*,*E*), but the eLTP was absent ($n = 6$: Fig. 5*C*,*D*), which indicates the involvement of NO downstream the astrocyte calcium signal. Because NO could be produced by both pyramidal neurons and astrocytes, to elucidate its source we included 100 μM L-NAME (an antagonist of the NO synthase that prevents NO production) in the recording pipette of the postsynaptic neuron and astrocytes to specifically prevent NO production in the postsynaptic cell and astrocyte local network, respectively (Fig. 5*A*,*D*). When L-NAME was included in the postsynaptic cell (L-NAME_N) the astrocyte $Ca^{2+}$ signal was unaffected ($n = 58$ astrocytes from $n = 5$ slices; Fig. 5*B*,*E*), but the paired depolarizing protocol did not induce long-term synaptic changes ($n = 5$; Fig. 5*C*,*D*). However, eLTP induced by pairing protocol was unaffected by previous loading of L-NAME into the astrocyte network (L-NAME_A; synaptic efficacy, Pr, and synaptic potency were 174.16 ± 32.1%,

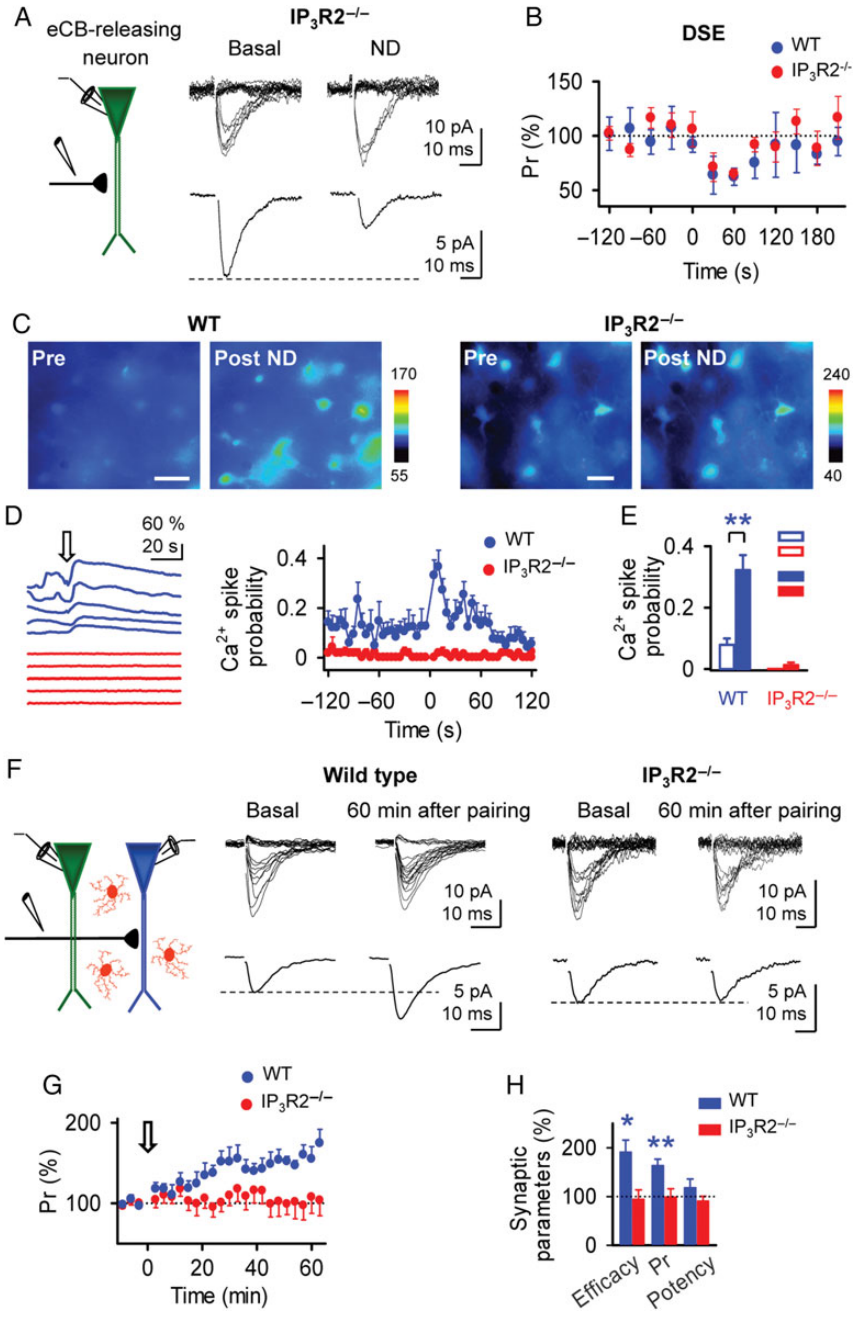


**Figure 3.** Endocannabinoid-induced LTP requires astrocyte $Ca^{2+}$ signal. (*A*) Representative synaptic responses (20 stimuli; top traces) and averaged EPSCs ($n = 20$ stimuli, including successes and failures; bottom traces) recorded from the eCB-releasing neuron before (basal) and after the neuronal depolarization (ND) to 0 mV in transgenic mouse $IP_3R2^{-/-}$. (*B*) Pr versus time in wild-type ($n = 6$) and $IP_3R2^{-/-}$ mice ($n = 6$). Note the similar depolarization-induced suppression of excitation (DSE; dots denote the average response of 30 s bins). (*C*) Pseudocolor images representing fluorescence intensities of fluo-4-filled astrocytes before (Pre) and after depolarizing the eCB-releasing neuron to 0 mV (Post ND) in wild-type and IP3R2$^{-/-}$ mice. Scale bar, 20 µm. (*D*) Left, representative astrocyte $Ca^{2+}$ responses to depolarization of the eCB-releasing neuron from 5 astrocytes shown in *C*. Right, astrocyte $Ca^{2+}$ spike probability versus time from wild-type and $IP_3R2^{-/-}$ mice (74 and 55 astrocytes from $n = 8$ and 8 slices, respectively). (*E*) Astrocyte $Ca^{2+}$ spike probability before (basal, open bars) and after depolarizing the eCB-releasing neuron to 0 mV in wild-type and $IP_3R2^{-/-}$ mice (filled bars; $n = 8$ and 8 slices, respectively). (*F*) Synaptic responses (20 stimuli; top traces) and averaged EPSCs ($n = 20$ stimuli, including successes and failures; bottom traces) recorded from the postsynaptic neuron before (basal) and 60 min after pairing protocol in slices from wild-type and $IP_3R2^{-/-}$ mice. (*G*) Pr versus time after pairing protocol in slices from wild-type ($n = 7$) and $IP_3R2^{-/-}$ mice ($n = 8$). (*H*) Relative changes of synaptic parameters 60 min after pairing protocol in wild-type ($n = 7$) and $IP_3R2^{-/-}$ mice ($n = 8$). $^*P < 0.05$, $^{**}P < 0.01$.

157.16 ± 20.5%, and 108.9 ± 11.9%, from baseline; $n = 11$; $P =$ 0.043, 0.018, and 0.47, respectively; Fig. 5*D*), indicating that NO synthesis from astrocytes does not contribute significantly to this form of synaptic plasticity. Taken together, these results indicate that in addition to the astrocyte $Ca^{2+}$ signal, NO production from postsynaptic cell during neuronal activity is required to generate eLTP.

To test whether NO was sufficient to induce eLTP without the involvement of additional postsynaptic signals, we directly supplied NO in the absence of postsynaptic depolarization, by pressure delivery (180 s) of the NO donor diethylamine NONOate (100 µM) from a micropipette (Fig. 5*A*). While NO donor application alone did not change synaptic transmission (synaptic efficacy, Pr, and synaptic potency were 97.7 ± 9.6%,

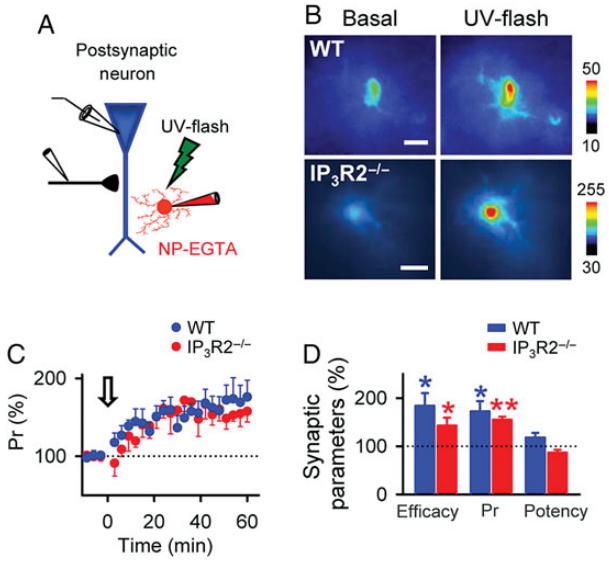


**Figure 4.** Pairing astrocyte stimulation and mild postsynaptic depolarization induces LTP in wild-type and $IP_3R2^{-/-}$ mice. (*A*) Schematic drawing depicting the recorded postsynaptic neuron and astrocyte filled with the $Ca^{2+}$-cage NP-EGTA. (*B*) Pseudocolor images representing fluorescence intensities of fluo-4-filled astrocytes before (basal) and after UV-light stimulation in wild-type and IP3R2$^{-/-}$ mice. Scale bar, 10 μm. (*C*) Pr versus time after pairing the UV-light stimulation and the mild postsynaptic depolarization (to −30 mV) in wild-type ($n = 6$) and $IP_3R2^{-/-}$ mice ($n = 6$). Zero time corresponds to the beginning of the paired stimuli (arrow). (*D*) Relative change of synaptic parameters 60 min after the paired stimuli in wild-type ($n = 6$) and $IP_3R2^{-/-}$ mice ($n = 6$). *$P < 0.05$, **$P < 0.01$.

102.9 ± 7.0%, and 99.8 ± 11.5%, from baseline; $n = 8$; $P = 0.581$, 0.989, and 0.689, respectively), pairing the NO delivery with the depolarization of the eCB-releasing neuron resulted in the generation of LTP in heteroneuronal synapses ($n = 9$; Fig. 5*C*, *D*). Taken together, these results confirm that NO produced by the postsynaptic neuron is the retrograde messenger involved in the eLTP.

We further investigated whether the co-release of NO and eCB by a single neuron could induce eLTP of synapses into that neuron (homosynapses). We then imposed the paired depolarizing protocol to the same neuron, that is the mild depolarization to −30 mV and to 0 mV for 5 s; but no changes in synaptic transmission were found in these neurons ($n = 9$; Fig. 5*D*). These data indicate that eLTP was independent of the spatial coincidence of eCB and NO signaling at the same synapses but it did depend on the temporal coincidence of both signals through astrocyte network activity.

### *Presynaptic Signaling: eLTP is Mediated by Activation of mGluRs and PKC in Presynaptic Terminals*

After the identification of the retrograde messenger originated from the postsynaptic neuron, we sought the presynaptic molecular mechanisms responsible for the eLTP. Because eLTP is mediated by eCB-induced stimulation of astrocytes, which release glutamate that regulates synaptic transmission through activation of mGluRs (Perea and Araque 2007; Navarrete and Araque 2010), we first investigated whether these receptors were involved in the eLTP. While in control conditions, the eLTP was induced by the paired depolarizing protocol (see Fig. 1), it was prevented in parallel experiments when slices were incubated with the antagonists of group I mGluRs MPEP (50 μM) and LY367385 (100 μM; mGluR5 and mGluR1 antagonists, respectively) ($n = 8$, synaptic efficacy change from basal values: 95.9 ± 15.9%; $P = 0.592$), without affecting the eCB-induced astrocyte $Ca^{2+}$ signal ($Ca^{2+}$ spike probability change from 0.04 ± 0.01 to 0.37 ± 0.08; $n = 53$ astrocytes from $n = 5$ slices, $P = 0.010$: cf. Navarrete and Araque 2010). In a subset of experiments without postsynaptic depolarization, DEA NONOate was applied in the presence of MPEP (50 μM) and LY367385 (100 μM) and no significant changes in synaptic efficacy were observed (111.7 ± 20.0% from basal values; $n = 11$; $P = 0.588$), suggesting that NO was not sufficient to induce eLTP, which also required mGluR1/5 receptor activation (Fig. 5*F*–*H*). We next investigated the subtype of mGluR involved by perfusing separately the group I mGluR antagonists (Fig. 6). While LY367385 abolished the eLTP (Fig. 6*A*–*C*) without modifying the astrocyte $Ca^{2+}$ signal (Fig. 6*D*,*E*), MPEP did not prevent eLTP (Fig. 6*B*,*C*), indicating that eLTP was specifically mediated by activation of mGluR1.

The changes in Pr and PPF indicate that eLTP is mediated by activation of presynaptic mGluRs. To test the possible contribution of postsynaptic mGluRs to the eLTP, we filled the postsynaptic neuron with Guanosine 5′-[β-thio]diphosphate (GDPβS, 2mM) to prevent mGluR-mediated signaling, as confirmed by the absence of calcium elevations evoked by local application of DHPG (2 mM; specific agonist of group I mGluRs) or acetylcholine (1 mM) (18 of 18 control neurons and 3 of 20 GDPβS-filled neurons showed calcium elevations) (Fig. 7*A*–*C*). In these conditions, paired stimulation still induced the potentiation of synaptic transmission (Fig. 7*D*–*F*). Additionally, in the presence of CB1 receptor antagonist AM251 and postsynaptic GDPβS, local application of DHPG, paired with postsynaptic depolarization to −30 mV was sufficient to induce eLTP (Fig. 7*G*–*I*). Although mGluR1/5 are largely located postsynaptically, present results indicate that eLTP was mediated by presynaptic rather than postsynaptic activation of these receptors.

However, no anatomical evidence exists for the presence of mGluRs at SC. We therefore performed immunoelectron microscopy studies using a pan-mGluR1 antibody, which recognizes an extracellular epitope common to all mGluR1 isoforms, and the pre-embedding immunogold method (Lujan et al. 1996), which allows the unambiguous localization at the plasma membrane of those subcellular compartments expressing the receptor. In a representative sample of asymmetrical synapses with CA1 pyramidal cells in the stratum radiatum (302 synapses from 3 animals), mGluR1 immunoparticles were found not only postsynaptically (57 synapses), but also at presynaptic sites (27 synapses) (Fig. 6*F*,*G*). Indeed, mGluR1 immunoparticles were found at both sites in a subset of synapses (11 of 27 synapses). These results provide anatomical evidence of the presence of mGluR1 in SC, confirming synaptic physiology data that indicate that eLTP results from activation of presynaptic mGluRs.

We then investigated the molecular target responsible for the long-term expression of the enhancement of synaptic transmitter release evoked by mGluR activation. Stimulation of mGluRs activates PKC, which is related with synaptic plasticity (for a review see Anwyl (2009)). Therefore, we tested different PKC inhibitors perfused in the bath or applied intracellularly in the postsynaptic neuron. The eLTP was prevented when the paired depolarizing protocol was delivered in the presence of 2 μM BIS I, a diffusible PKC inhibitor (Toullec et al. 1991; Daw et al. 2000) that can act pre- or postsynaptically ($n = 4$, Fig. 8*A*, *B*), and that did not modify the eCB-induced astrocyte $Ca^{2+}$

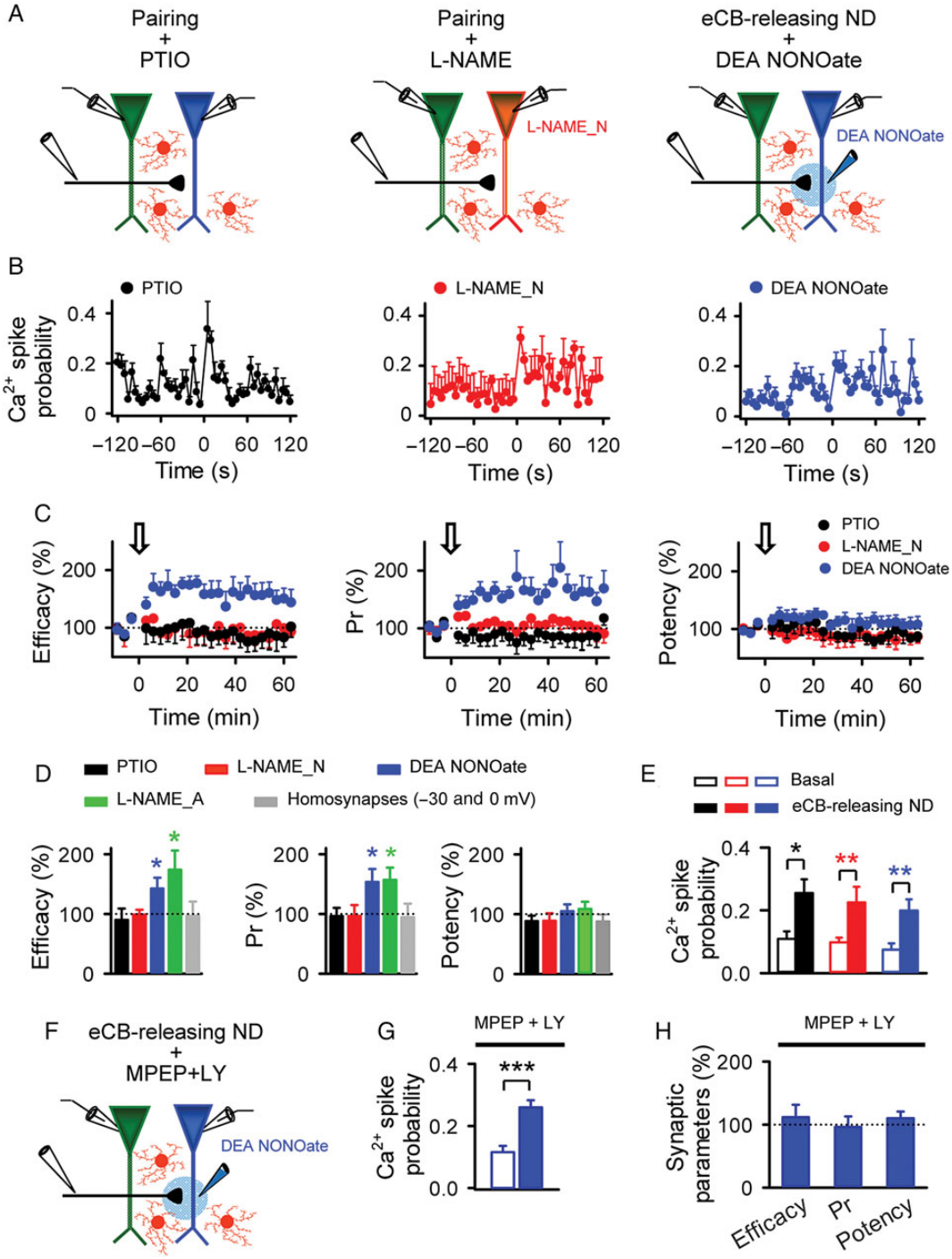


**Figure 5.** Endocannabinoid-induced LTP depends on postsynaptic nitric oxide production. (*A*) Schematic drawing depicting the experimental conditions: paired depolarizing protocol in the presence of 100 μM PTIO (left) or after loading the postsynaptic neuron with 100 μM L-NAME (center; L-NAME_N), and paring eCB-releasing neuronal depolarization to 0 mV with a puff of 100 μM DEA NONOate (right). (*B*) Astrocyte $Ca^{2+}$ spike probability versus time in each condition (left to right: $n = 7$, 5, and 11 slices, respectively). Zero time corresponds to the beginning of the eCB-releasing neuronal depolarization. (*C*) Synaptic parameters versus time in presence of PTIO ($n = 6$), postsynaptic L-NAME_N ($n = 5$), and DEA NONOate ($n = 9$). (*D*) Relative changes of synaptic parameters 60 min after stimuli in presence of PTIO, postsynaptic L-NAME_N, L-NAME_A (astrocytes loading with L-NAME; $n = 11$), DEA NONOate, and pairing protocol (−30 and 0 mV) in single neuron (homosynapses; $n = 9$). (*E*) Basal and maximum astrocyte $Ca^{2+}$ spike probability in the presence of PTIO (black), postsynaptic L-NAME_N (red), and DEA NONOate (blue). (*F*) Schematic drawing depicting paired recordings and a puff of 100 μM DEA NONOate in the presence of group I mGluR antagonists, MPEP, and LY367385. (*G*) Basal and maximum astrocyte $Ca^{2+}$ spike probability evoked by eCB-releasing neuronal depolarization in the presence of MPEP and LY367385 (86 astrocytes from $n = 9$ slices). (*H*) Relative changes of synaptic parameters before and 60 min after pairing a DEA NONOate puff with the depolarization of the eCB-releasing neuron in the presence of MPEP and LY367385 ($n = 11$). $^*P < 0.05$, $^{**}P < 0.01$, $^{***}P < 0.001$.

elevations ($n = 58$ astrocytes from $n = 6$ slices) (Fig. 8*C*). In contrast, eLTP was still present when the PKC inhibitor chelerythrine (1 μM; (Ling et al. 2002; Kwon and Castillo 2008) was included in the postsynaptic neuron through the recording pipette ($n = 9$, Fig. 8*A*,*B*). The effectiveness of chelerythrine was assessed in parallel experiments by monitoring the slow

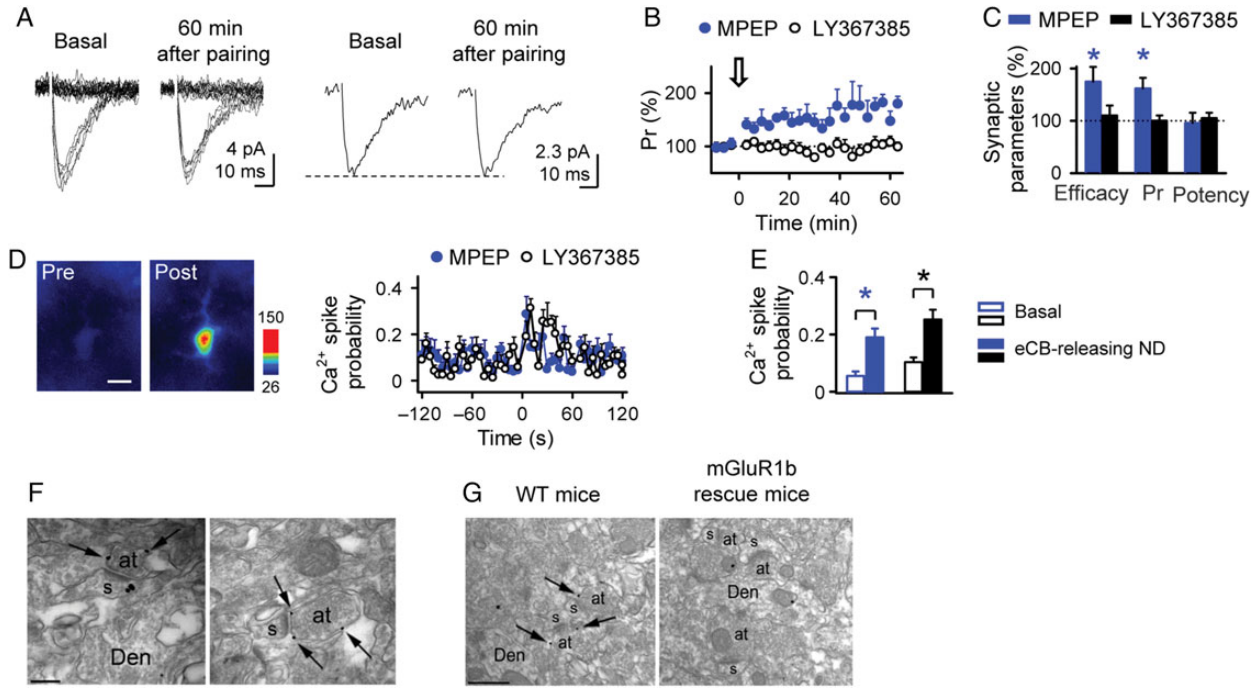


**Figure 6.** Endocannabinoid-induced LTP is mediated by presynaptic mGluRs type 1. (*A*) Representative synaptic responses (20 stimuli; left traces) and averaged EPSCs (20 stimuli, including successes and failures; right traces) recorded from the postsynaptic neuron before (basal) and 60 min after pairing protocol in the presence of LY367385 (100 μM). (*B*) Pr versus time in the presence of MPEP and LY367385 ($n = 6$ and $n = 12$, respectively). Zero time corresponds to the beginning of the paired depolarizing protocol. (*C*) Relative change of synaptic parameters 60 min after pairing protocol in MPEP and LY367385 ($n = 6$ and $n = 12$, respectively). (*D*) Pseudocolor images representing fluorescence intensities of a fluo-4-filled astrocyte before (Pre) and after depolarizing the eCB-releasing neuron to 0 mV (Post) in the presence of LY367385. Scale bar, 10 μm. Astrocyte $Ca^{2+}$ spike probability versus time in the presence of MPEP and LY367385 (64 astrocytes, $n = 7$ slices and 91 astrocytes, $n = 6$ slices, respectively). Zero time corresponds to the beginning of the eCB-releasing neuronal depolarization. (*E*) Basal and maximum astrocyte $Ca^{2+}$ spike probability in the presence of MPEP and LY367385. (*F*) Electron micrographs of the CA1 hippocampal region showing immunoparticles for mGluR1 in the stratum radiatum. Immunoparticles for mGluR1 were located at presynaptic sites along the plasma membrane (arrows) of excitatory axon terminals (at) establishing asymmetrical synapses with dendritic spines (s) of CA1 pyramidal cells. Den, dendritic shafts of pyramidal cell. Scale bar, 0.2 μm. (*G*) Characterization of the pan-mGluR1 antibody immunoparticles for mGluR1 in WT animal (left panel), and mGluR1b rescue mice (right panel). Left, few immunogold particles for mGluR1 were detected at presynaptic sites along the plasma membrane (arrows) of excitatory axon terminals (at) in the stratum radiatum, presumably Schaffer's collaterals, always outside the active zone. Right, immunogold particles for mGluR1 were never detected at presynaptic sites, but only occasionally on mitochondria or myelinated axons. Den, dendritic shaft; s, dendritic spine. Scale bar, 0.5 μm. $^*P < 0.05$.

$Ca^{2+}$-activated $K^+$ current ($sI_{AHP}$), which is sensitive to PKC activation (Engisch et al. 1996; Dutar and Nicoll 1988; Seroussi et al. 2002). We performed paired recordings with one neuron filled with control solution and the other neuron filled with the intracellular solution containing 1-μM chelerythrine (Fig. 8*D*). While bath application of the PKC activator PMA (phorbol 12-myristate 13-acetate, 15 μM) (Engisch et al. 1996) inhibited the $sI_{AHP}$ in control neurons; the $sI_{AHP}$ was unaffected in the chelerythrine-filled neurons ($n = 4$; Fig. 8*E*,*F*). Taken together, these results indicate that activation of PKC and mGluRs, located presynaptically rather than postsynaptically, mediate the long-term enhancement of presynaptic transmitter release.

## Discussion

Present results show that eCBs released from pyramidal neurons, in addition to their well-known effects suppressing synaptic activity, can induce long-term enhancement of synaptic transmission through activation of astrocytes. eCB-astrocyte signaling potentiates the probability of transmitter release in heteroneuronal synapses when the eCB-evoked astrocyte $Ca^{2+}$ signal coincides with postsynaptic activity. In addition, these data show the transmitters and molecular pathways involved in this eLTP, which results from the concerted activity of the 3 elements of the tripartite synapse, that is, the eCB-evoked astrocyte $Ca^{2+}$ signal that stimulates the gliotransmitter release of glutamate, the NO production from the postsynaptic neuron, and the activation of presynaptic mGluRs and PKC signaling (Fig. 8*G*).

The effects of eCB signaling on synaptic transmission and plasticity has been studied in different brain areas, where it has been found to induce inhibition of neurotransmitter release through activation of presynaptic CB1Rs, which leads to different forms of short-term and long-term depression, such as DSI, DSE, or LTD (e.g., Kreitzer and Regehr 2001a; Alger 2002; Wilson and Nicoll 2002; Freund et al. 2003; Chevaleyre et al. 2006; Heifets and Castillo 2009; Navarrete and Araque 2010). Present results demonstrate that eCBs can trigger LTP of synaptic transmission in the hippocampus through stimulation of astrocytes. They reveal that eCBs, which are largely considered a retrograde signal that evokes synaptic depression, may also serve as a lateral signal through activation of astrocytes that lead to synaptic transmission enhancement in synapses relatively distant from the eCB source, that is, heteroneuronal synapses. Therefore, present findings indicate that eCBs can exert additional effects to classical synaptic depression, which is also supported by recent reports in mice and rats (Navarrete and Araque 2010; Xu et al. 2012; Tamagnini et al. 2013), goldfish Mauthner cell synapses (Cachope et al. 2007), and synapses in the spinal locomotor network of the lamprey (Song et al.

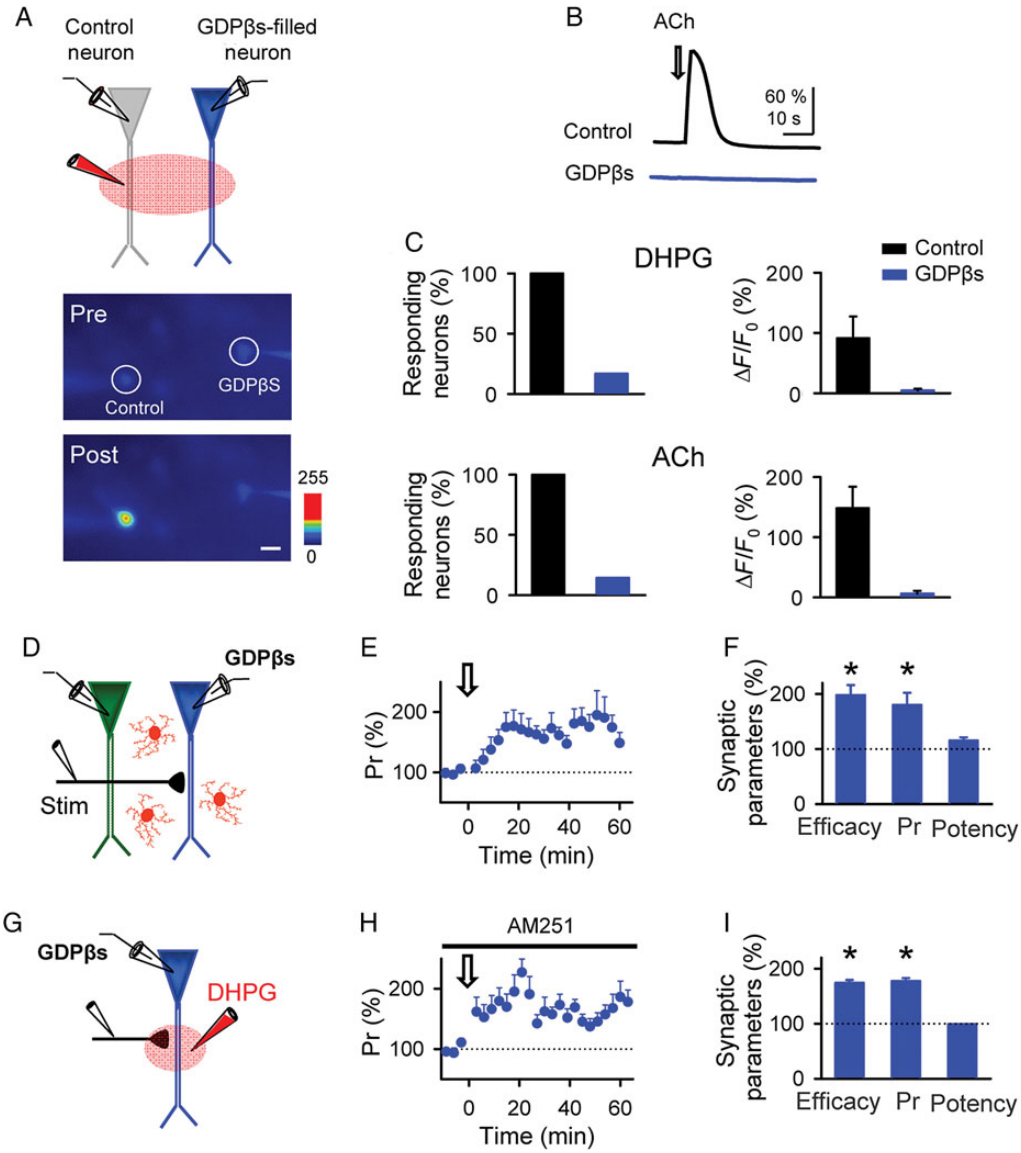


**Figure 7.** Presynaptic locus of astrocyte-mediated endocannabinoid-induced LTP. (*A*) Top, schematic drawing of the experimental approach depicting GDPβS dialysis into the postsynaptic neuron. Bottom, pseudocolor images representing fluorescence intensities of a fluo-4-filled neuron (Control) and a GDPβS–fluo-4-filled neuron (GDPβS) before (Pre) and after (Post) a puff application of ACh. Scale bar 20 μm. (*B*) Time course of the $Ca^{2+}$ response of the cells indicated in *A*. (*C*) Number of control and GDPβS-filled neurons showing a $Ca^{2+}$ increase evoke by DHPG (top, $n = 7$ and 6, respectively) and Ach (bottom, $n = 11$ and 14, respectively). (*D*) Schematic drawing of the experimental approach depicting paired recordings in the presence of postsynaptic GDPβS. (*E*) Pr versus time before and after the paired depolarizing protocol in GDPβS-filled postsynaptic neuron ($n = 9$). Zero time corresponds to the beginning of the paired depolarizing protocol. (*F*) Relative changes of synaptic parameters 60 min after the paired depolarizing protocol in GDPβS-filled postsynaptic neurons ($n = 9$). (*G*) Schematic drawing of the experimental approach depicting the pairing of a puff of 300 μM DHPG with a mild depolarization of the GDPβS-filled postsynaptic neuron in the presence of AM251 (2 μM). (*H*) Pr versus time before and after the puff of DHPG in the presence of AM251 ($n = 10$). Zero time corresponds to the beginning of the puff of DHPG. (*I*) Relative changes of synaptic parameters 60 min after puff application of DHPG in the presence of AM251 ($n = 10$). *$P < 0.05$.

2012). The fact that eCBs may have opposite effects on neurotransmission reveals a higher complexity of eCB signaling on synaptic transmission regulation than previously thought. They may have relevant implications in network function because the opposite effects of eCBs on synaptic transmission are spatially defined and depend on the target cells. Indeed, while eCBs are known to lead to transient or LTD through activation of presynaptic CB1Rs in homoneuronal synapses close to the eCB source (<20 μm) (Wilson and Nicoll 2001; Chevaleyre and Castillo 2004; Chevaleyre et al. 2006; Navarrete and Araque 2010), they transiently (Navarrete and Araque 2010) or persistently (present results) potentiate synaptic transmission at more distant synapses through activation of astrocytes. Homoneuronal synapses may be influenced by the neuronal NO release and the eCB-induced astrocytic glutamate signaling triggered by the neuronal depolarization; however, these synapses exhibit synaptic depression induced by eCBs released from the eCB-releasing neuron (see Fig. 3*A*,*B*; cf. Kreitzer and Regehr 2001b; Ohno-Shosaku et al. 2001; Chevaleyre et al. 2006; Navarrete and Araque 2010). In contrast, heteroneuronal synapses, which are more distant from the short-range eCB signaling direct effect, display the persistent synaptic potentiation due to the coordinated activity of astrocytic mGluR and neuronal NO signaling pathways. Thus, the final outcome of this complex and spatially controlled signaling is that astrocytes selectively "feed forward" to the adjacent

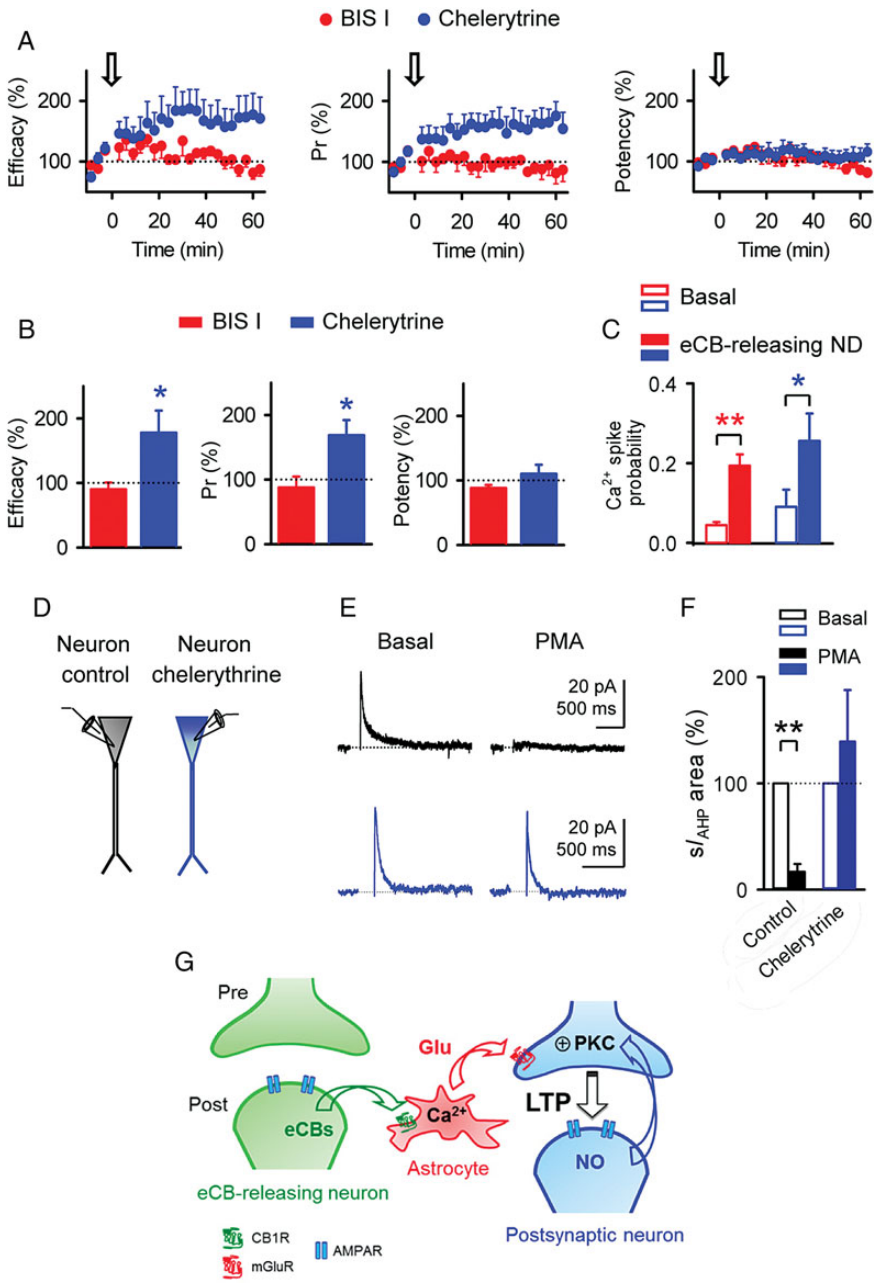


**Figure 8.** Endocannabinoid-induced LTP is mediated by PKC activation. (*A*) Synaptic parameters versus time in the presence of PKC inhibitor BIS I (2 μM) and after loading the postsynaptic neuron with 1 μM chelerytrine ($n = 4$ and 9, respectively). Zero time corresponds to the beginning of the paired depolarizing protocol. (*B*) Relative change of synaptic parameters 60 min after the paired depolarizing protocol in the presence of BIS I and chelerytrine ($n = 4$ and 9, respectively). (*C*) Basal and maximum astrocyte $Ca^{2+}$ spike probability in the presence of BIS I and chelerytrine (58 and 46 astrocytes from $n = 6$ and 6 slices, respectively). (*D*) Schematic drawing depicting a control neuron and a neuron filled with chelerythrine. (*E*) Representative traces showing the $sI_{AHP}$ evoked by 200 ms depolarizing pulses before and 20 min after perfusion with PMA (15 μM), in a control neuron (black traces) and in a chelerythrine-filled neuron (blue traces). (*F*) Relative changes of $sI_{AHP}$ area in each condition ($n = 4$). (*G*) Schematic drawing representing the signaling pathways involved in the endocannabinoid-induced hippocampal lateral LTP. $^*P < 0.05$, $^{**}P < 0.01$.

neurons, but do not "feedback" to the eCB-releasing neuron, because the direct activation of presynaptic CB1Rs by eCBs leads to synaptic depression, which overpowers the mGluR-mediated signaling that would lead to eLTP (cf. (Navarrete and Araque 2010). Consequently, eCBs released from active neurons depress neurotransmission in close synapses; while simultaneously lead to lateral potentiation of more distant synapses, generating a core/shell spatial arrangement of synaptic depression/potentiation.

We show that eCB-induced LTP necessarily requires the involvement of astrocytes, which play an essential role by responding to eCBs with $Ca^{2+}$ elevations and stimulating glutamate release, thus expanding the original signal to more distant points and transforming it into a potentiating signal. While the role of astrocyte $Ca^{2+}$ and gliotransmission has been questioned by recent reports based on negative results obtained using transgenic mice (Fiacco et al. 2007; Petravicz et al. 2008; Agulhon et al. 2010), including $IP_3R2^{-/-}$ mice that in the present study showed an impairment of the eLTP, our data support a high physiological relevance of these phenomena on synaptic function (e.g., Haydon and Carmignoto 2006; Jourdain et al. 2007; Perea and Araque 2007; Di Castro et al. 2011;

Panatier et al. 2011; Navarrete et al. 2012). Therefore, present results further support the tripartite synapse concept, showing that astrocytes are actively involved in synaptic transmission and plasticity, exerting relevant roles in synaptic function, being able to spatially extend intercellular signals and to transform the sign of the effects of intercellular messengers. Furthermore, present study provides further evidence to the accumulating data showing the contribution of astrocytes to synaptic plasticity (Martineau et al. 2006; Panatier et al. 2006; Perea and Araque 2007; Henneberger et al. 2010; Takata et al. 2011; Min and Nevian 2012; Navarrete et al. 2012), indicating that astrocytes are actively involved in storage information in the brain.

The coincidence of the astrocyte $Ca^{2+}$ signal evoked by $Ca^{2+}$ uncaging and postsynaptic activity has been previously shown to lead to the generation of hippocampal LTP (Perea and Araque 2007). Our present results indicate that the astrocyte-mediated LTP can be triggered by an endogenous stimulus (i.e., eCBs released form neurons) that physiologically elevates $Ca^{2+}$ in astrocytes. Cholinergic-evoked $Ca^{2+}$ elevations in astrocytes have been reported to mediate cholinergic-induced hippocampal LTP (Navarrete et al. 2012). Because astrocytes express a wide variety of G protein-coupled receptors that can mobilize intracellular calcium, whether different neurotransmitters may trigger similar mechanisms for LTP may have a strong impact on our current understanding of the signaling mechanisms that can lead to LTP. Additionally, present results identified the molecular mechanisms and signaling pathways involved in the astrocyte-mediated LTP. We show that astrocyte CB1Rs activated by eCBs elevate $Ca^{2+}$ and stimulate glutamate release that acting on type I mGluRs persistently enhance synaptic transmitter release when it coincides with a postsynaptic signal (i.e., NO), through activation of presynaptic PKC. mGluR-dependent LTP is known to occur in different areas of the brain including the neocortex, hippocampus, striatum, and nucleus accumbens (for a review see Anwyl (2009)). Present results are consistent with the mechanisms proposed to mediate mGluR-mediated LTP, but our data further reveal that astrocytes are the source of glutamate responsible for the generation of eLTP.

The eCB-induced LTP requires activation of group I mGluRs by glutamate released from astrocytes after being stimulated by eCBs. The subcellular localization of these mGluRs is not fully elucidated. Although these mGluRs can be located at postsynaptic sites (Lujan et al. 1996), physiological data indicate that these mGluRs are located presynaptically because: 1) eLTP is characterized by the enhancement of transmitter release probability without changes in synaptic potency, which indicates a presynaptic rather than a postsynaptic underlying mechanism (Fig. 1*E*); and 2) eLTP is associated with changes in the PPF (Fig. 1*C*), which is consistent with a presynaptic mechanism. Additional electrophysiological studies also suggest the existence of presynaptic mGluRs in SC, where they can regulate synaptic transmission (e.g., Rodriguez-Moreno et al. 1998; Fiacco and McCarthy 2004; Sanchez-Prieto et al. 2004; Perea and Araque 2007; Navarrete and Araque 2010; Bonansco et al. 2011; Navarrete et al. 2012). Besides this compelling physiological evidence, we show for the first time, to our knowledge, morphological evidence at the ultrastructural level of the presence of group I mGluRs at SC presynaptic terminals. Furthermore, because mGluR1a is located exclusively at postsynaptic sites in asymmetrical synapses between CA1 pyramidal cells and SC (Lujan et al. 1996), the presynaptic localization of mGluR1 is likely due to the presence of the 1b isoform. Interestingly, because synaptic potentiation has been described to occur only when these receptors are activated by exogenous glutamate or glutamate released from astrocytes, perhaps they are exclusively activated by gliotransmitters and therefore are specific molecular targets of astrocyte–neuron signaling.

In summary, we present evidence indicating that eCBs can induce LTP through the necessary involvement of astrocyte activity and gliotransmitter release, and revealing the different signaling pathways at cellular and molecular level underlying this eLTP, such as the interaction between pyramidal cells and astrocytes, and the eCBs, mGluR, NO, and PKC signaling. While eCBs are considered retrograde signals that depress neurotransmission, we show that they lead to a more distant regulation of synaptic activity inducing a lateral potentiation through activation of astrocytes. This eCB-induced LTP requires the coordinated activity of the 3 elements of the tripartite synapse: astrocyte gliotransmission, postsynaptic activity, and presynaptic activation of mGluRs. Our results show a novel mechanism that reconciles the previous results regarding the NO and eCB signaling role in LTP (Schuman and Madison 1991; Carlson et al. 2002; Crosby et al. 2011; Hardingham et al. 2013) and astrocyte-mediated plasticity (Panatier et al. 2006; Perea and Araque 2007; Henneberger et al. 2010; Takata et al. 2011; Navarrete et al. 2012). The effects on synaptic modulation by eCBs are spatially defined, establishing a core of synaptic depression in close synapses to the eCB source surrounded by a shell of synaptic potentiation in more distant synapses. Because present results were obtained in juvenile mice, it is possible that the described mechanisms correspond to specific events occurring during development. Further studies are required to evaluate whether astrocyte-induced eLTP is a general phenomenon also present in adults, where the expression of some signaling molecules involved might be downregulated.

Hence, these results reveal novel mechanisms underlying the consequences of eCB signaling as well as astrocyte activity on hippocampal synaptic plasticity, and may affect to the physiological roles of eCB system in learning and memory processes in particular, and in the overall brain function.

## Funding

This work was supported by grants from Ministerio de Economia y Competitividad, Spain (MINECO; BFU2010-15832), European Union (HEALTH-F2-2007-202167), and Cajal Blue Brain to A.A. Grants from Spain (MINECO; BFU-2009-08404 and CSD2008-00005) to R.L. Grants from Spain (MINECO; Consolider, CSD2010-00045; Ramón y Cajal Program, RYC-2012-12014; and BFU2013-47265) to G.P.

## Notes

The authors declare no competing financial interests. We thank Dr Atsu Aiba (Animal Resources, Center for Disease Biology and Integrative Medicine, Faculty of Medicine, University of Tokyo) for the donation of the mGluR1b rescue mice. *Conflict of Interest*: None declared.

## References

Agulhon C, Fiacco TA, McCarthy KD. 2010. Hippocampal short- and long-term plasticity are not modulated by astrocyte Ca2+ signaling. Science. 327(5970):1250–1254.

Alger BE. 2002. Retrograde signaling in the regulation of synaptic transmission: focus on endocannabinoids. Prog Neurobiol. 68 (4):247–286.
Anwyl R. 2009. Metabotropic glutamate receptor-dependent long-term potentiation. Neuropharmacology. 56(4):735–740.
Araque A, Carmignoto G, Haydon PG. 2001. Dynamic signaling between astrocytes and neurons. Annu Rev Physiol. 63:795–813.
Araque A, Martin ED, Perea G, Arellano JI, Buño W. 2002. Synaptically released acetylcholine evokes Ca2+ elevations in astrocytes in hippocampal slices. J Neurosci. 22(7):2443–2450.
Araque A, Parpura V, Sanzgiri RP, Haydon PG. 1999. Tripartite synapses: glia, the unacknowledged partner. Trends Neurosci. 22(5):208–215.
Bonansco C, Couve A, Perea G, Ferradas CA, Roncagliolo M, Fuenzalida M. 2011. Glutamate released spontaneously from astrocytes sets the threshold for synaptic plasticity. Eur J Neurosci. 33 (8):1483–1492.
Cachope R, Mackie K, Triller A, O'Brien J, Pereda AE. 2007. Potentiation of electrical and chemical synaptic transmission mediated by endocannabinoids. Neuron. 56(6):1034–1047.
Carlson G, Wang Y, Alger BE. 2002. Endocannabinoids facilitate the induction of LTP in the hippocampus. Nat Neurosci. 5(8):723–724.
Chevaleyre V, Castillo PE. 2004. Endocannabinoid-mediated metaplasticity in the hippocampus. Neuron. 43(6):871–881.
Chevaleyre V, Takahashi KA, Castillo PE. 2006. Endocannabinoid-mediated synaptic plasticity in the CNS. Annu Rev Neurosci. 29:37–76.
Crosby KM, Inoue W, Pittman QJ, Bains JS. 2011. Endocannabinoids gate state-dependent plasticity of synaptic inhibition in feeding circuits. Neuron. 71(3):529–541.
Daw MI, Chittajallu R, Bortolotto ZA, Dev KK, Duprat F, Henley JM, Collingridge GL, Isaac JT. 2000. PDZ proteins interacting with C-terminal GluR2/3 are involved in a PKC-dependent regulation of AMPA receptors at hippocampal synapses. Neuron. 28(3):873–886.
Di Castro MA, Chuquet J, Liaudet N, Bhaukaurally K, Santello M, Bouvier D, Tiret P, Volterra A. 2011. Local Ca2+ detection and modulation of synaptic release by astrocytes. Nat Neurosci. 14(10):1276–1284.
Dutar P, Nicoll RA. 1988. Classification of muscarinic responses in hippocampus in terms of receptor subtypes and second-messenger systems: electrophysiological studies in vitro. J Neurosci. 8(11):4214–4224.
Engisch KL, Wagner JJ, Alger BE. 1996. Whole-cell voltage-clamp investigation of the role of PKC in muscarinic inhibition of IAHP in rat CA1 hippocampal neurons. Hippocampus. 6(2):183–191.
Fiacco TA, McCarthy KD. 2004. Intracellular astrocyte calcium waves in situ increase the frequency of spontaneous AMPA receptor currents in CA1 pyramidal neurons. J Neurosci. 24(3):722–732.
Fiacco TA, Agulhon C, Taves SR, Petravicz J, Casper KB, Dong X, Chen J, McCarthy KD. 2007. Selective stimulation of astrocyte calcium in situ does not affect neuronal excitatory synaptic activity. Neuron. 54(4):611–626.
Freund TF, Katona I, Piomelli D. 2003. Role of endogenous cannabinoids in synaptic signaling. Physiol Rev. 83(3):1017–1066.
Han J, Kesner P, Metna-Laurent M, Duan T, Xu L, Georges F, Koehl M, Abrous DN, Mendizabal-Zubiaga J, Grandes P et al. 2012. Acute cannabinoids impair working memory through astroglial CB1 receptor modulation of hippocampal LTD. Cell. 148(5):1039–1050.
Hardingham N, Dachtler J, Fox K. 2013. The role of nitric oxide in presynaptic plasticity and homeostasis. Front Cell Neurosci. 7:190.
Hawkins RD, Son H, Arancio O. 1998. Nitric oxide as a retrograde messenger during long-term potentiation in hippocampus. Prog Brain Res. 118:155–172.
Haydon PG, Carmignoto G. 2006. Astrocyte control of synaptic transmission and neurovascular coupling. Physiol Rev. 86(3):1009–1031.
Heifets BD, Castillo PE. 2009. Endocannabinoid signaling and long-term synaptic plasticity. Annu Rev Physiol. 71:283–306.
Henneberger C, Papouin T, Oliet SH, Rusakov DA. 2010. Long-term potentiation depends on release of D-serine from astrocytes. Nature. 463(7278):232–236.
Isaac JT, Hjelmstad GO, Nicoll RA, Malenka RC. 1996. Long-term potentiation at single fiber inputs to hippocampal CA1 pyramidal cells. Proc Natl Acad Sci USA. 93(16):8710–8715.
Jourdain P, Bergersen LH, Bhaukaurally K, Bezzi P, Santello M, Domercq M, Matute C, Tonello F, Gundersen V, Volterra A. 2007. Glutamate exocytosis from astrocytes controls synaptic strength. Nat Neurosci. 10(3):331–339.
Kang J, Jiang L, Goldman SA, Nedergaard M. 1998. Astrocyte-mediated potentiation of inhibitory synaptic transmission. Nat Neurosci. 1 (8):683–692.
Kishimoto Y, Fujimichi R, Araishi K, Kawahara S, Kano M, Aiba A, Kirino Y. 2002. mGluR1 in cerebellar Purkinje cells is required for normal association of temporally contiguous stimuli in classical conditioning. Eur J Neurosci. 16(12):2416–2424.
Kreitzer AC, Regehr WG. 2001b. Cerebellar depolarization-induced suppression of inhibition is mediated by endogenous cannabinoids. J Neurosci. 21(20):RC174.
Kreitzer AC, Regehr WG. 2001a. Retrograde inhibition of presynaptic calcium influx by endogenous cannabinoids at excitatory synapses onto Purkinje cells. Neuron. 29(3):717–727.
Kwon HB, Castillo PE. 2008. Long-term potentiation selectively expressed by NMDA receptors at hippocampal mossy fiber synapses. Neuron. 57(1):108–120.
Li X, Zima AV, Sheikh F, Blatter LA, Chen J. 2005. Endothelin-1-induced arrhythmogenic Ca2+ signaling is abolished in atrial myocytes of inositol-1,4,5-trisphosphate(IP3)-receptor type 2-deficient mice. Circ Res. 96(12):1274–1281.
Ling DS, Benardo LS, Serrano PA, Blace N, Kelly MT, Crary JF, Sacktor TC. 2002. Protein kinase Mzeta is necessary and sufficient for LTP maintenance. Nat Neurosci. 5(4):295–296.
Lujan R, Nusser Z, Roberts JD, Shigemoto R, Somogyi P. 1996. Perisynaptic location of metabotropic glutamate receptors mGluR1 and mGluR5 on dendrites and dendritic spines in the rat hippocampus. Eur J Neurosci. 8(7):1488–1500.
Maldonado R, Valverde O, Berrendero F. 2006. Involvement of the endocannabinoid system in drug addiction. Trends Neurosci. 29 (4):225–232.
Martin ED, Araque A, Buno W. 2001. Synaptic regulation of the slow Ca2+-activated K+ current in hippocampal CA1 pyramidal neurons: implication in epileptogenesis. J Neurophysiol. 86(6):2878–2886.
Martineau M, Baux G, Mothet JP. 2006. D-serine signalling in the brain: friend and foe. Trends Neurosci. 29(8):481–491.
Min R, Nevian T. 2012. Astrocyte signaling controls spike timing-dependent depression at neocortical synapses. Nat Neurosci. 15 (5):746–753.
Navarrete M, Araque A. 2008. Endocannabinoids mediate neuron-astrocyte communication. Neuron. 57(6):883–893.
Navarrete M, Araque A. 2010. Endocannabinoids potentiate synaptic transmission through stimulation of astrocytes. Neuron. 68(1):113–126.
Navarrete M, Perea G, Fernandez de Sevilla D, Gómez-Gonzalo M, Núñez A, Martín ED, Araque A. 2012. Astrocytes mediate in vivo cholinergic-induced synaptic plasticity. PLoS Biol. 10(2):e1001259.
Nedergaard M, Ransom B, Goldman SA. 2003. New roles for astrocytes: redefining the functional architecture of the brain. Trends Neurosci. 26(10):523–530.
Nett WJ, Oloff SH, McCarthy KD. 2002. Hippocampal astrocytes in situ exhibit calcium oscillations that occur independent of neuronal activity. J Neurophysiol. 87(1):528–537.
Ohno-Shosaku T, Maejima T, Kano M. 2001. Endogenous cannabinoids mediate retrograde signals from depolarized postsynaptic neurons to presynaptic terminals. Neuron. 29(3):729–738.
Ohno-Shosaku T, Tsubokawa H, Mizushima I, Yoneda N, Zimmer A, Kano M. 2002. Presynaptic cannabinoid sensitivity is a major determinant of depolarization-induced retrograde suppression at hippocampal synapses. J Neurosci. 22(10):3864–3872.
Panatier A, Vallée J, Haber M, Murai KK, Lacaille JC, Robitaille R. 2011. Astrocytes are endogenous regulators of basal transmission at central synapses. Cell. 146(5):785–798.
Panatier A, Theodosis DT, Mothet JP, Touquet B, Pollegioni L, Poulain DA, Oliet SH. 2006. Glia-derived D-serine controls NMDA receptor activity and synaptic memory. Cell. 125(4):775–784.
Parpura V, Zorec R. 2010. Gliotransmission: exocytotic release from astrocytes. Brain Res Rev. 63(1–2):83–92.
Parri HR, Gould TM, Crunelli V. 2001. Spontaneous astrocytic Ca2+ oscillations in situ drive NMDAR-mediated neuronal excitation. Nat Neurosci. 4(8):803–812.

Perea G, Araque A. 2007. Astrocytes potentiate transmitter release at single hippocampal synapses. Science. 317(5841):1083–1086.
Perea G, Araque A. 2005. Properties of synaptically evoked astrocyte calcium signal reveal synaptic information processing by astrocytes. J Neurosci. 25(9):2192–2203.
Perea G, Navarrete M, Araque A. 2009. Tripartite synapses: astrocytes process and control synaptic information. Trends Neurosci. 32 (8):421–431.
Petravicz J, Fiacco TA, McCarthy KD. 2008. Loss of IP3 receptor-dependent Ca2+ increases in hippocampal astrocytes does not affect baseline CA1 pyramidal neuron synaptic activity. J Neurosci. 28(19):4967–4973.
Piomelli D. 2003. The molecular logic of endocannabinoid signalling. Nat Rev Neurosci. 4(11):873–884.
Raastad M. 1995. Extracellular activation of unitary excitatory synapses between hippocampal CA3 and CA1 pyramidal cells. Eur J Neurosci. 7(9):1882–1888.
Rodriguez-Moreno A, Sistiaga A, Lerma J, Sánchez-Prieto J. 1998. Switch from facilitation to inhibition of excitatory synaptic transmission by group I mGluR desensitization. Neuron. 21(6):1477–1486.
Sanchez-Prieto J, Paternain AV, Lerma J. 2004. Dual signaling by mGluR5a results in bi-directional modulation of N-type Ca2+ channels. FEBS Lett. 576(3):428–432.
Schuman EM, Madison DV. 1994. Nitric oxide and synaptic function. Annu Rev Neurosci. 17:153–183.
Schuman EM, Madison DV. 1991. A requirement for the intercellular messenger nitric oxide in long-term potentiation. Science. 254 (5037):1503–1506.
Seroussi Y, Brosh I, Barkai E. 2002. Learning-induced reduction in post-burst after-hyperpolarization (AHP) is mediated by activation of PKC. Eur J Neurosci. 16(5):965–969.
Singh P, Jorgačevski J, Kreft M, Grubišić V, Stout RF Jr, Potokar M, Parpura V, Zorec R. 2014. Single-vesicle architecture of synaptobrevin2 in astrocytes. Nat Commun. 5:3780.
Song J, Kyriakatos A, El Manira A. 2012. Gating the polarity of endocannabinoid-mediated synaptic plasticity by nitric oxide in the spinal locomotor network. J Neurosci. 32(15):5097–5105.
Takata N, Mishima T, Hisatsune C, Nagai T, Ebisui E, Mikoshiba K, Hirase H. 2011. Astrocyte calcium signaling transforms cholinergic modulation to cortical plasticity in vivo. J Neurosci. 31(49):18155–18165.
Tamagnini F, Barker G, Warburton EC, Burattini C, Aicardi G, Bashir ZI. 2013. Nitric oxide-dependent long-term depression but not endocannabinoid-mediated long-term potentiation is crucial for visual recognition memory. J Physiol. 591(Pt 16):3963–3979.
Toullec D, Pianetti P, Coste H, Bellevergue P, Grand-Perret T, Ajakane M, Baudet V, Boissin P, Boursier E, Loriolle F et al. 1991. The bisindolylmaleimide GF 109203X is a potent and selective inhibitor of protein kinase C. J Biol Chem. 266(24):15771–15781.
Volterra A, Meldolesi J. 2005. Astrocytes, from brain glue to communication elements: the revolution continues. Nat Rev Neurosci. 6 (8):626–640.
Wilson RI, Nicoll RA. 2002. Endocannabinoid signaling in the brain. Science. 296(5568):678–682.
Wilson RI, Nicoll RA. 2001. Endogenous cannabinoids mediate retrograde signalling at hippocampal synapses. Nature. 410(6828):588–592.
Xu JY, Zhang J, Chen C. 2012. Long-lasting potentiation of hippocampal synaptic transmission by direct cortical input is mediated via endocannabinoids. J Physiol. 590(Pt 10):2305–2315.
Zimmer A, Zimmer AM, Hohmann AG, Herkenham M, Bonner TI. 1999. Increased mortality, hypoactivity, and hypoalgesia in cannabinoid CB1 receptor knockout mice. Proc Natl Acad Sci USA. 96 (10):5780–5785.